Design and Evolution of an Opto-electronic Device for VOCs Detection

Ana Carolina Pádua[1], Susana Palma[1], Jonas Gruber[2], Hugo Gamboa[3] and Ana Cecília Roque[1]
[1]*UCIBIO, REQUIMTE, Departamento de Química, Faculdade de Ciências e Tecnologia da Universidade NOVA de Lisboa, 2829-516 Caparica, Portugal*
[2]*Departamento de Química Fundamental, Instituto de Química da Universidade de São Paulo, Av. Prof. Lineu Prestes, 748 CEP 05508-000, São Paulo, SP, Brasil*
[3]*Laboratório de Instrumentação Engenharia Biomédica e Física da Radiação (LIBPhys-UNL), Departamento de Física, Faculdade de Ciências e Tecnologia da Universidade NOVA de Lisboa, Monte da Caparica, 2829-516 Caparica, Portugal*

Keywords: Device, Electronic-nose, Gas Sensing, Volatile Organic Compounds.

Abstract: Electronic noses (E-noses) are devices capable of detecting and identifying Volatile Organic Compounds (VOCs) in a simple and fast method. In this work, we present the development process of an opto-electronic device based on sensing films that have unique stimuli-responsive properties, altering their optical and electrical properties, when interacting with VOCs. This interaction results in optical and electrical signals that can be collected, and further processed and analysed. Two versions of the device were designed and assembled. E-nose V1 is an optical device, and E-nose V2 is a hybrid opto-electronic device. Both E-noses architectures include a delivery system, a detection chamber, and a transduction system. After the validation of the E-nose V1 prototype, the E-nose V2 was implemented, resulting in an easy-to-handle, miniaturized and stable device. Results from E-nose V2 indicated optical signals reproducibility, and the possibility of coupling the electrical signals to the optical response for VOCs sensing.

1 INTRODUCTION

The interest in odours detection is common in several areas, namely in food quality, environmental protection, and medical diagnosis. Volatile organic compounds (VOCs) can be regarded as indicators of food spoilage, presence of hazardous gases in the air, and even certain diseases when found in some biological samples.

Electronic noses (E-noses) can be used to detect and identify VOCs in a fast and automated manner. Since their invention (Wilkens and Hartman, 1964), many were developed and optimized for diverse applications (Zohora et al., 2016). During the 80s, E-noses were defined as instruments which included an array of heterogeneous electrochemical gas sensors with partial specificity and a pattern recognition system (Persaud and Dodd, 1982; Llobet et al., 1999). However, this definition has been broadening along the time. In the last years, the term E-nose has been used to mention gas sensors that alter their properties, in consequence of changes in a gaseous atmosphere.

Generally, the E-noses architecture is similar to the human olfactory system (Gutierrez and Horrillo, 2014). They comprise of a delivery system that transfers the air to be analysed from the headspace of a sample chamber to a detection chamber, like the air circulating in the nasal cavities; Inside the detection chamber, an array of heterogeneous gas sensors with partial specificity and selectivity mimics the odorant receptors, and their interaction with the VOCs; and a signal processing unit with pattern recognition methods have the same function that the olfactory bulb and the brain have in odours recognition.

Currently, there are some commercial products based on E-nose technology, suitable for a wide range of applications. For instance, *The eNose company* is mainly focused on applications for medical research, namely for differentiating head and neck carcinoma from lung carcinoma (van Hooren et al., 2016), and for diagnosis of bacterial and viral infections in obstructive pulmonary disease (van Geffen, Bruins and Kerstjens, 2016). *Breathtec Biomedical, Inc.* is interested in early screening of diseases such

Pádua, A., Palma, S., Gruber, J., Gamboa, H. and Roque, A.
Design and Evolution of an Opto-electronic Device for VOCs Detection.
DOI: 10.5220/0006558100480055
In *Proceedings of the 11th International Joint Conference on Biomedical Engineering Systems and Technologies (BIOSTEC 2018) - Volume 1: BIODEVICES*, pages 48-55
ISBN: 978-989-758-277-6

as cancer, tuberculosis, and diabetes. *Peres* offers a product to evaluate food quality. *Sensigent*, *Sacmi*, and *AIRSENSE Analytics* developed very versatile E-noses for environmental protection, security screening and quality control that benefit from the use of customizable sensor modules, and pattern recognition methods based on machine learning algorithms. *Nano Mobile Healthcare* is developing a technology from *NASA*, not only for aerospace safety, but also for medical diagnosis and road security. And, *CSIRO* is creating a biosensor with numerous possible applications.

The sizes of commercial E-noses range from desktop, to laptop or hand size. The sensing materials also vary, being the most common metal oxides (Barsan, Koziej and Weimar, 2007; Mirzaei, Leonardi and Neri, 2016), and polymers (Li, 2009). Other arrays based on metals (Gutmacher et al., 2011), nanoporous pigments/dyes (Feng et al., 2010), nanostructures (Jing Kong et al., 2000) and liquid crystals (Boden et al., 1999) have also been used for gas sensing.

2 SENSING MATERIALS

Our research group has developed a new class of sensing gels for gas sensing. These materials possess enormous versatility and have unique stimuli-responsive properties, altering their optical and electrical properties when interacting with VOCs (Hussain et al., 2017). The sensing gels are composed of liquid crystal (LC) droplets self-assembled in the presence of ionic liquid, dispersed inside a biopolymer matrix.

The way the sensing gels alter their optical properties relies on the way light propagates through nematic liquid crystals, which typically produce a 90-degree shift in light polarisation. Hence, having the sensing films sandwiched between two crossed polarising filters, it is possible to observe changes in light polarisation, when in the presence or absence of VOCs.

Light-emitting diodes (LEDs) are sources of unpolarised light. When the emitted light passes through the first polariser, only light polarised along the y-axis can pass. Next, the light passes through the second polariser (called the analyser), which only allows light polarised along the x-axis to pass. Therefore, the light that pass through the analyser is minimal, since there is negligible light polarised along the x-axis emerging from the polariser.

However, if a glass slide with the sensing gel spread on it (which has nematic LC in its composition) is placed between the polariser and the analyser, the anisotropy of the nematic LC, produces a shift in the light polarised along the y-axis (that comes from the first polariser). This way, part of that light becomes polarised along the x-axis. Therefore, the light can pass though the analyser, and be detected by the light-dependent-resistor (LDR) - Figure 1 (a).

In the presence of VOCs, the LCs change their configuration from radial to isotropic. Thus, the light polarised along the y-axis, even passing through the gel, maintains the polarisation, and so is blocked by the analyser - Figure 1 (b). Hence, minimal light intensity reaches the LDR.

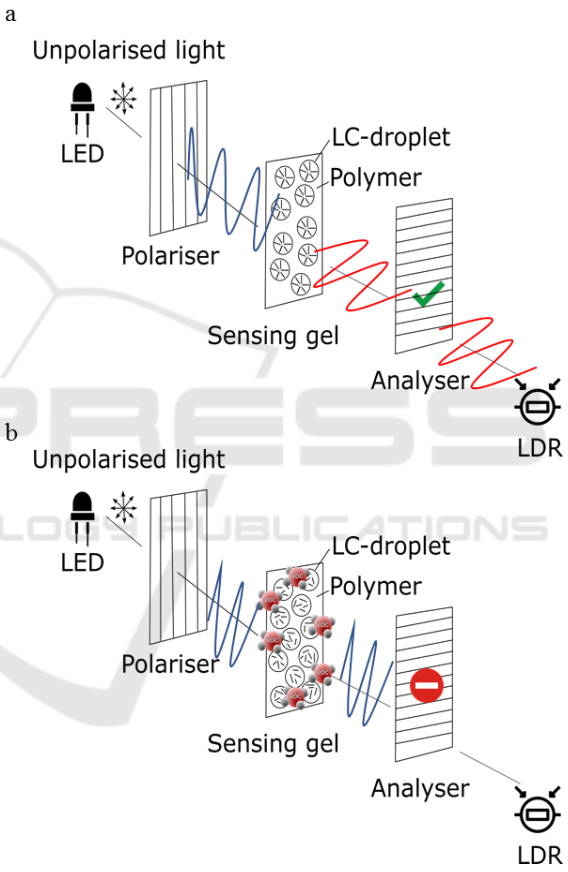

Figure 1: (a) The light emitted by the LED achieves the LDR when no VOCs are interacting with the sensing gel; (b) and is blocked when VOCs are interacting with the sensing gel.

Regarding the electrical effects, the sensing gels exhibit high conductivity in the absence of VOCs. On the contrary, when interacting with VOCs their conductivity decreases (Hussain et al., 2017).

To explore the application of these gels for gas sensing, our research group is developing an electronic nose (E-nose). If the interaction dynamics of distinct VOCs with the sensing gels vary, different

optical and electrical signals will be obtained. This brings the possibility of VOCs detection and identification in a simple and rapid manner. The final goal is to achieve an accurate, miniaturized and scalable device that could run the analysis automatically.

3 DESIGN AND ASSEMBLY OF DEVICE VERSIONS

The first prototype of E-nose, called the E-nose V0, is shown in Figure 2 (a). The apparatus is composed of a detection chamber, a delivery system, and a transduction system.

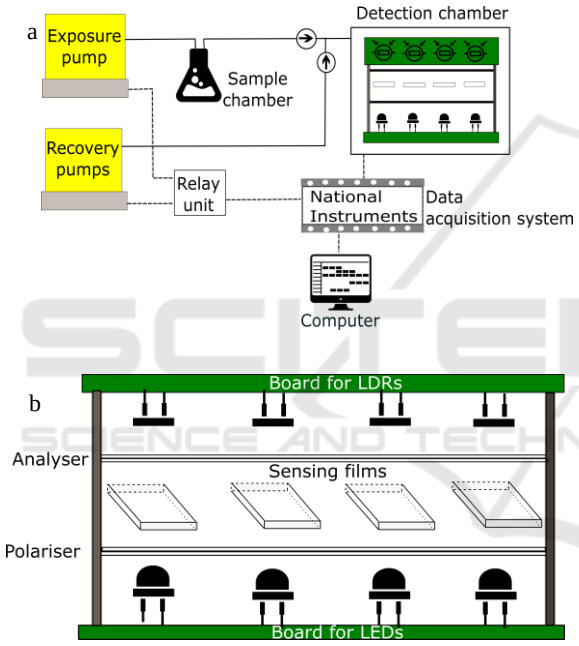

Figure 2: (a) Schematic of E-nose V0 and (b) detection chamber.

The delivery system includes the air pumps (exposure and recovery pumps), the sample chamber, tubes and connectors, and two non-return valves to prevent back-flow. The Exposure pump is responsible for carrying the VOCs from the sample chamber (where is the chemical solution) to the detection chamber. Therefore, it is ON in the exposure periods and OFF in the recovery periods. The recovery system is composed of two air pumps which clean the detection chamber, making the atmospheric air circulate through the chamber, and removing the VOCs. Some tubes were longer than necessary, which resulted in higher exposure and recovery times required for the experiments. Moreover, the area of the liquid-gas surface inside the sample chamber was changing for different volumes of solvent, due to its tapered configuration.

The detection chamber – Figure 2 (b) - is the E-nose component where the VOCs interact with the sensing materials. It contains an array of four optical sensors able to detect those interactions. For each optical sensor, the unpolarised light emitted by the LED pass through a sensing film sandwiched between two crossed polarising filters (polariser and analyser), and finally reaches the photo detector. Photo resistors, photo diodes or photo transistors could have been used as photo detectors. Our choice was the use of light dependent resistors (whose resistance decrease with increasing incident light) because they are the most commonly used photo detectors, and could be used in a very simple circuit (based on voltage dividers). Moreover, LDRs are cheap, readily available in many sizes and shapes, and need low power and voltage for operation. Regarding the electronic components, since the LEDs and LDRs have some variations inherent to their own production, signals calibration is an important issue. Additionally, interference between optical sensors was observed in the signals response, because the LDRs of the optical pairs were not only receiving light from the LED in front, but also from the LEDs in the surroundings. Variations in the sensing films' exposed areas to light also resulted in unstable responses, given that the sensing gels were not homogeneously spread over all the parts of the glass slides. The first prototype also suffered difficulties to handle and it had air leaks in the tube connectors.

The transduction system was based on a *National Instruments* board, which acquired the data generated by the LDRs. The collected signals were sent to a computer and could be visualized in a LabVIEW interface. Additionally, the exposure and recovery times were defined as LabVIEW inputs. The board used a 5 V to trigger the relay switch unit, which in turn determined the exposure and recovery pump states. In some situations, the noise was too high, inhibiting the observation of the sensor response. Besides, the hardware and software used were both expensive. We concluded that the construction of a new cheaper and controllable transduction system could help solving these problems.

3.1 Optical E-nose V1

The schematic of the optical E-nose V1, which resulted from improvements made in E-nose V0, is represented in Figure 3.

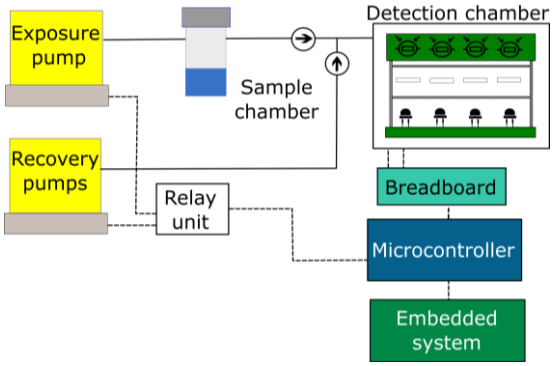

Figure 3: Schematic of E-nose V1.

A new detection chamber, easier to handle, was assembled for E-nose V1. Inside it, the interference between optical sensors was minimized.

Opaque mask's layers – Figure 4 (a) - were implemented to prevent the interference of dispersed light from neighbour LEDs with each LDR response. Given that the sensing gels on the glass slides were not homogeneously spread, opaque black masks – Figure 4 (b) - were applied on the back of the glass slides. This delimitates the area of gel exposed.

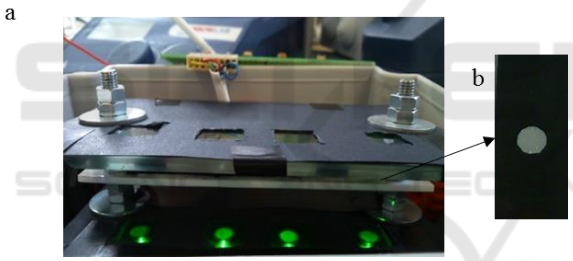

Figure 4: (a) Opaque masks layers implemented to prevent the interference of dispersed light from the LEDs in the surroundings with the LDRs response. (b) Sensing film with an opaque mask applied.

A new hermetic sample chamber with a cylindrical configuration was implemented. This way, the area of the liquid-gas surface is the same, independently of the volume used. In the pipelines, shorter silicone tubes and polypropylene connectors were used. Having shorter tubes, lower recovery and exposure periods were required.

The transduction system previously implemented in E-nose V0 was not scalable, because the data acquisition system was expensive, and required cable connection to a computer. Thus, for E-nose V1, the transduction system was redesigned. The new system uses an Arduino Uno (a microcontroller) and a Raspberry Pi 2 Model B (an embedded system), that can be remotely controlled by a computer. Since the transduction system was implemented using open-source hardware and software, it became two orders of magnitude cheaper than the previous version. Currently, it is an autonomous unit, the mechanisms for data visualization and data analysis are faster, and a scalable architecture was achieved.

3.2 Hybrid E-nose V2

The new E-nose implemented should fulfill some requirements: it should be stable, miniaturized, and easy to handle. Moreover, it should enable less time needed for experiments, and to test more sensing films simultaneously. Having these goals in mind, the E-nose V2 was designed according to the schematic shown in Figure 5. This E-nose is hybrid, since the optical detection chamber can be easily replaced by an electrical sensors chamber.

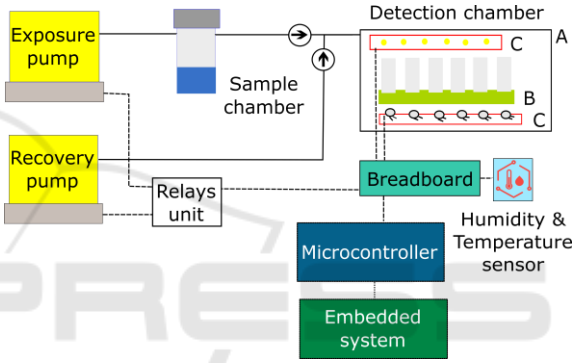

Figure 5: Schematic of the E-nose V2.

The delivery system is composed of an exposure and a recovery pumps. It has also a sample chamber, tubes, connectors, and non-return valves similar to the ones used in E-nose V1.

The transduction system is a replica of the E-nose V1, based on Arduino Due and Raspberry Pi 2 Model B. Arduino Due was used, because it has twelve analog input pins, whereas Arduino Uno has only six.

A humidity and temperature sensor was included in the E-nose instrumentation to measure the room conditions. And, the relays switch unit was wired to the microcontroller and pumps.

3.2.1 Optical Detection Chamber

The optical detection chamber is composed of: an opaque external box - Figure 5 A) - that protects the optical sensors from the interference of environmental light; an internal support for sensing films with a glass chamber on it to concentrate the VOCs near the sensing films - Figure 5 B); Printed Circuit Boards (PCBs) - Figure 5 C) - for the emission

circuit – Figure 6 (a) - and for the detection circuit Figure 6 (b).

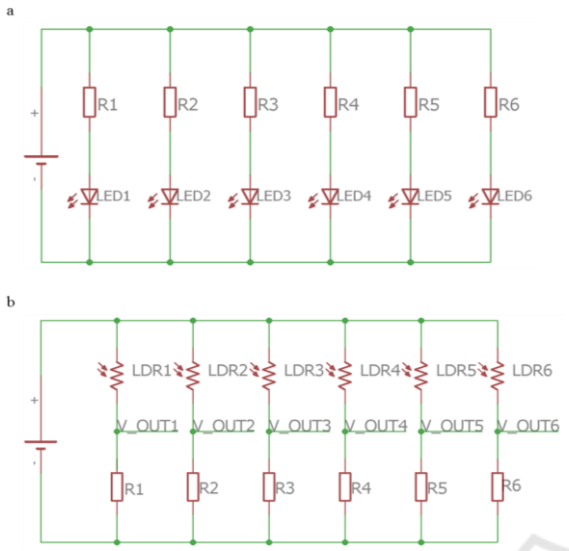

Figure 6: Schematic of the (a) emission circuit and (b) detection circuit of E-nose V2 PCBs.

Inside the E-nose V2 detection chamber, six LEDs/LDRs were placed in parallel, instead of four used in E-nose V1. Another difference is that the LDRs power supply is 3.3 V, because an analog input value higher than 3.3 V may damage the Arduino Due. The components used in the PCBs are through-hole technology mounting type.

3.2.2 Electrical Detection Chamber

For testing the sensing films electrical response, the detection chamber should be replaced by the electrical sensors chamber. This consists of a little box with capacity for an array of 8 interdigitated electrodes inside. The sensing films exhibit capacitive effects. To avoid accumulation of charges in the electrical films, they can be continuously polarised and depolarised, using alternating current (AC).

The method used to detect the changes that occur in the electrical sensors while interacting with the VOCs requires the use of a conductivity meter installed between the Arduino and the detection chamber. The conductivity meter implemented is described in (da Rocha et al., 1997). An oscillator generates a triangular wave, that is applied to one of the electrode terminals. The other terminal is wired to the input of a current-to-voltage converter. After rectification and filtering, the output voltage becomes proportional to the conductance in the electrode.

4 RESULTS

4.1 Signals Calibration

The optical sensors were calibrated for each LED/LDR pair, according to the following equation:

$$\text{Calibrated signal} = \frac{s - \min}{\max - min} \quad (1)$$

s – signal values obtained (V). The value is given by the LDR, when a sensing film is sandwiched between two crossed polarising filters, in the absence - Figure 1 (a) - or presence of VOCs - Figure 1 (b).

min – average of signal values obtained when two crossed polarising filters are placed between the LED and the LDR. Without placing the sensing gel in the middle, the light intensity that reaches the LDR is minimal. Therefore, given the LDR response curve, its resistance will be maximum. Consequently, according to the Ohm's law, the voltage drop at the LDR will be maximum. Yet, taking in account the LDR schematic shown in Figure 6 (b), the analog output signal V_{out} (detected by the Arduino) is given by:

$$V_{out} = V_R = V_{Source} - V_{LDR} \quad (2)$$

Thus, if the voltage drop at the LDR is maximum, the output voltage will be minimum.

max – average of signal values obtained when two parallel polarising filters are placed between the LED and the LDR (without sensing gel in the middle). The light intensity that reaches the LDR is maximum. Therefore, its resistance will be minimum. Consequently, the voltage drop will be minimum. According to equation 2, if the voltage drop at the LDR is minimum, the output voltage will be maximum.

The calibration signals, from which the min and max are calculated, are obtained without placing any sensing film between the two polarising filters. The experiments are performed inside the detection chamber, with the LEDs ON. Each E-nose (V1 or optical V2) only needs a single calibration, before the first experiment, and not in the beginning of each experiment. Each E-nose unit requires its own calibration, and cannot use calibration values from other E-noses, because the rationale behind calibration is to compensate differences among LEDs and LDRs inherent to their production.

4.2 Optical Signals Evolution

Examples of optical signals obtained in E-nose V0, V1 and V2 are shown in Figure 7. A significative

improvement in the signal to noise ratio can be observed from E-nose V0, to E-noses V1 and V2.

From E-nose V1 to E-nose V2, the exposure and recovery times were reduced for 1/10. This was possible due to the miniaturized detection chamber implemented in E-nose V2. The total chamber volume was reduced from 1200 mL (in V1) to 20 mL (in V2). Consequently, the E-nose V2 allows acquisition of more data in less time.

4.3 Signals Obtained

To evaluate if the E-nose V1 could detect vapors of different organic solvents, several optical sensing films were prepared. 60 µL of sensing gel were spread over microscope glass slides cut with dimensions 40 mm x 15 mm.

3 tests were conducted in the E-nose V1, using the conditions: 5 mL of organic solvent inside the sample chamber, heated at 36 °C. The room temperature was set to 20 °C. The room humidity ranged from 46 % to 87 %. The exposure time was 50 s, and the recovery time was 150 s. The total duration was 15 min. And, the sampling rate was 10 Hz.

Test 1, 2 and 3 included 13 experiments, each one using different organic solvents, namely acetone, carbon tetrachloride, chloroform, dichloromethane, diethyl ether, isopropanol, ethanol, ethyl acetate, heptane, hexane, methanol, toluene and xylene. The results obtained for acetone, carbon tetrachloride, hexane, and methanol are shown in Figure 8.

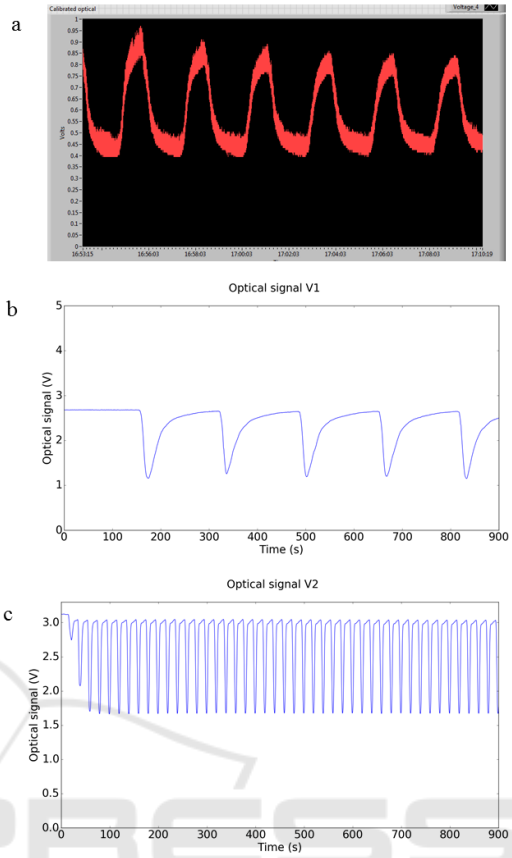

Figure 7: Evolution of optical signals from (a) E-nose V0 to (b) E-nose V1 and (c) E-nose V2. The gas sample used was atmospheric air saturated in acetone for all the plots.

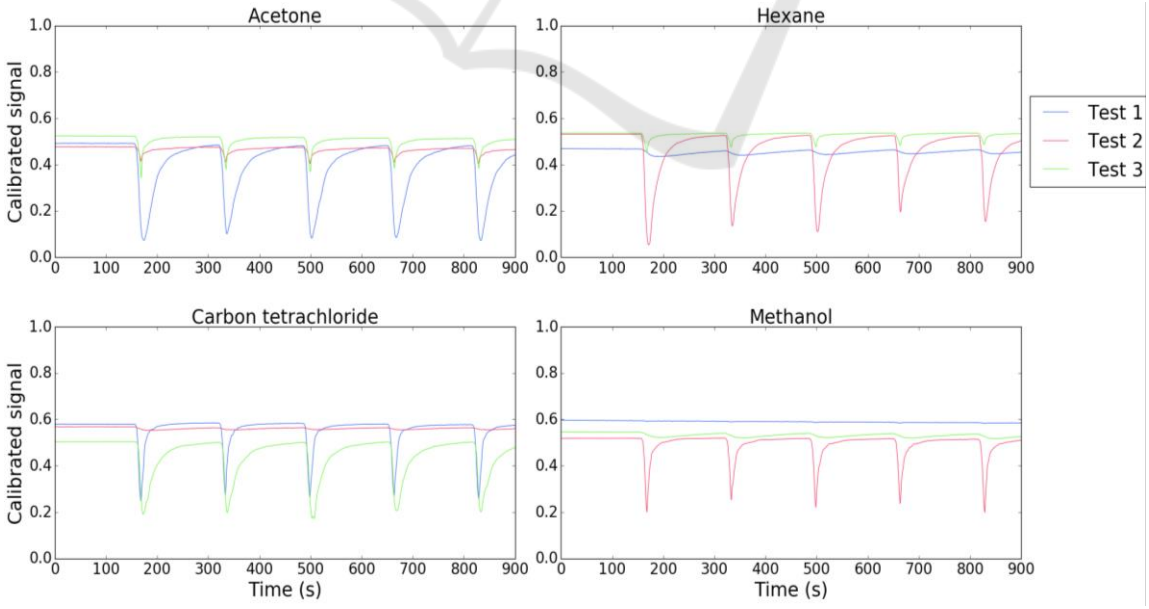

Figure 8: Optical signals obtained using the same sensing film exposed to different VOCs in test 1, test 2 and test 3, using E-nose V1. The sensing films were composed of 1-butyl-3-methylimidazolium dicyanamide [BMIM] [DCA], 4-Cyano-4'-pentylbiphenyl (5CB), Bovine Skin Gelatine (BSG), Sorbitol, and Milli-Q water (Hussain *et al.*, 2017).

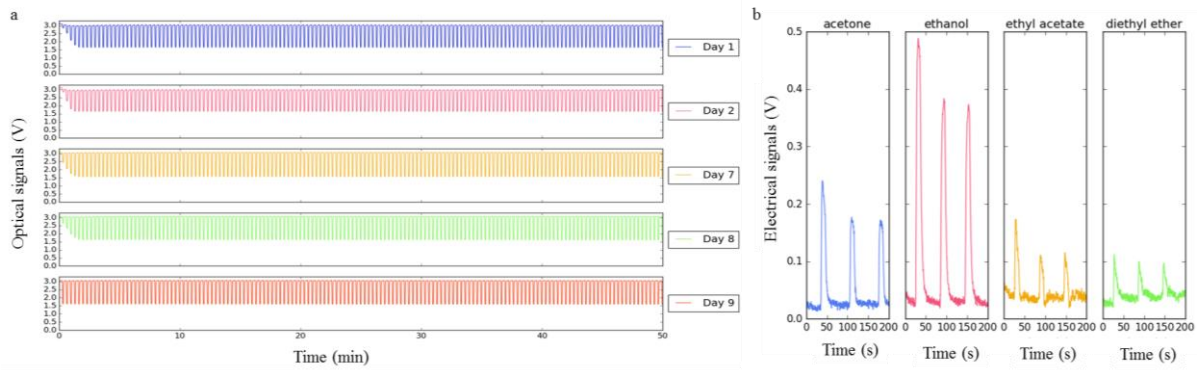

Figure 9: (a) Optical signals obtained using the same sensing film cyclically exposed to acetone along 10 days. The sensing films were composed of [BMIM] [DCA], 5CB, BSG, and Milli-Q water (Hussain *et al.*, 2017). (b) Electrical signals obtained using the same sensing film for different VOCs exposure. The electrical films were composed of [BMIM] [DCA], 5CB, BSG, Sorbitol, and Milli-Q water (Hussain *et al.*, 2017).

One can observe that for the same test (test 1, 2 or 3) the interaction of the sensing gels with different VOCs originates signals with different features. This is an indicator that the device might be useful for VOCs distinction and identification.

However, observing the signals for each VOC, we can identify significant differences comparing the results from test 1, test 2 and test 3. Thus, we can conclude that the results were not reproducible for different tests. Possible reasons for lack of reproducibility can be: the sensing films spreading method was not adequate; the device was not stable enough, because it was difficult to place the sensing films at the same position for different tests; and the LDRs PCB had to be taken out and placed again for different tests, due to E-nose V1 horizontal configuration.

To solve these issues, the E-nose V2 was assembled, and a reproducibility test was conducted. An array of six sensing films with the same composition was placed inside the detection chamber, and kept at the same position for 10 days.

The experimental conditions were: 5 mL of acetone inside the sample chamber, at 36 °C. The room temperature was 21-23 °C. The room humidity ranged from 58 % to 89 %. The exposure time was 5 s, and the recovery time was 15 s. The total duration was 50 min. And, the sampling rate was 5 Hz.

Two of the six sensing films tested originated reproducible responses along the 10 days. Figure 9 (a) shows a reproducible response given by one of them.

To test the electrical response, interdigitated electrodes 0.2 mm were prepared, spreading 15 µL of the sensing gel over each one. The sensing gel composition tested that gave an electrical response for several VOCs – see Figure 9 (b) - is described in the caption of this Figure. The conditions used in the experiment were: 5 mL of the organic solvent inside the sample chamber, at 37 °C. The exposure time was 10 s, and the recovery time was 50 s. The total duration was 4 min.

5 CONCLUSIONS

Regarding the device evolution, the E-nose V2 is more stable, miniaturized, and controllable than E-nose V1. The detection chamber of E-nose V2 was miniaturized, and consequently the exposure and recovery times required for VOCs detection were reduced. It is easier to handle, because it has a vertical configuration, while E-nose V1 has a horizontal one. Thus, in E-nose V2, the sensing films can be easily placed and removed. Also, the chamber is more stable because the sensing films are placed in fixed positions. Nevertheless, more improvements are needed to get close to a commercial product: a hermetic detection chamber should be implemented; and, the LED and photo detector of each optical pair should be perfectly aligned. This can be achieved using PCBs with surface-mount technology components. For future versions, photo diodes or photo transistors should be tested to substitute the LDRs, because they might have better performance-to-cost ratio, sensitivity and stability for this application. Besides, their response speed is faster.

The humidity and temperature sensors installed in E-nose V2 might add valuable information about the influence of the room conditions in the sensing films response. We intend to study that correlation in detail soon. For the transduction system, the signals

response must be normalized, and several classification methods can be explored.

Furthermore, small, lightweight and low-power pumps can be used in future versions of the device, so it can achieve portability without the need of an electric generator.

In what concerns to the electrical part, the conductivity meter architecture should be re-designed to be simpler and easily scalable. For instance, the possibility of generating an input digital wave should be explored. In addition, the electrodes finishing surface should be more corrosion-resistant (the use of nickel and gold, or platinum might be a solution). The duration of the experiments related to the electrical signals should be longer, allowing the study of the response at different measurement intervals, to improve quantification and interpretation of results.

The studies performed so far intend to characterize the device, identify its limitations, and optimize the technology. That is why, the tests were performed successively in cycles during several minutes. Nevertheless, our vision is to achieve a device that gives a response in the range of seconds.

The final goal is to accomplish a portable and user-friendly device. Accuracy, stability, and scalability are imperative to get to an E-nose, that can be explored towards several applications in environmental protection, security, product quality, or medical research.

ACKNOWLEDGMENTS

This work was supported by the European Research Council (SCENT-ERC-2014-STG-639123) and UCIBIO, financed by FCT/MEC (UID/Multi/04378/2013) and co-financed by the ERDF under the PT2020 Partnership Agreement (POCI-01-0145-FEDER-007728). The authors thank FCT/MEC for the research fellowship PD/BD/105752/2014 for A.P. The authors also acknowledge funding from CNPq, Brazil (400740/2014-1).

REFERENCES

Barsan, N., Koziej, D. and Weimar, U. (2007) 'Metal oxide-based gas sensor research: How to?', *Sensors and Actuators B: Chemical*, 121(1), pp. 18–35.

Boden, N. *et al.* (1999) 'Device applications of charge transport in discotic liquid crystals', *Journal of Materials Chemistry*, 9, pp. 2081–2086.

Feng, L. *et al.* (2010) 'A colorimetric sensor array for identification of toxic gases below permissible exposure limits', *Chemical Communications*, (12), pp. 2037–2039.

van Geffen, W. H., Bruins, M. and Kerstjens, H. A. M. (2016) 'Diagnosing viral and bacterial respiratory infections in acute COPD exacerbations by an electronic nose: a pilot study.', *Journal of breath research*. IOP Publishing, 10(3), p. 36001.

Gutierrez, J. and Horrillo, M. C. (2014) *Advances in artificial olfaction: Sensors and applications*, *Talanta*. doi: 10.1016/j.talanta.2014.02.016.

Gutmacher, D. *et al.* (2011) 'Comparison of gas sensor technologies for fire gas detection', *Procedia Engineering*. Elsevier B.V., 25, pp. 1121–1124.

van Hooren, M. R. A. *et al.* (2016) 'Differentiating head and neck carcinoma from lung carcinoma with an electronic nose: a proof of concept study', *European Archives of Oto-Rhino-Laryngology*, 273(11), pp. 3897–3903.

Hussain, A. *et al.* (2017) 'Tunable Gas Sensing Gels by Cooperative Assembly', *Advanced Functional Materials*, 27(27), pp. 1–14. Available at: http://dx.doi.org/10.1002/adfm.201700803.

Jing Kong, author *et al.* (2000) 'Nanotube Molecular Wires as Chemical Sensors', 287(5453 OP-Science. 287(5453):622-625), p. 622.

Li, S. (2009) *Overview of Odor Detection Instrumentation and the Potential for Human Odor Detection in Air Matrices*. MITRE Nano.

Llobet, E. *et al.* (1999) 'Fuzzy ARTMAP based electronic nose data analysis', *Sensors & Actuators: B. Chemical*, 61(1 OP), pp. 183–190.

Mirzaei, A., Leonardi, S. G. and Neri, G. (2016) 'Detection of hazardous volatile organic compounds (VOCs) by metal oxide nanostructures-based gas sensors: A review', *Ceramics International*. Elsevier, 42(14), pp. 15119–15141. doi: 10.1016/j.ceramint.2016.06.145.

Persaud, K. and Dodd, G. (1982) 'Analysis of discrimination mechanisms in the mammalian olfactory system using a model nose.', *Nature*, 299(5881), pp. 352–5.

da Rocha, R. T., Gutz, I. G. R. and do Lago, C. L. (1997) 'A Low-Cost and High-Performance Conductivity Meter', *Journal of Chemical Education*. American Chemical Society, 74(5), p. 572. Available at: http://dx.doi.org/10.1021/ed074p572.

Wilkens, W. F. and Hartman, J. D. (1964) 'An electronic analog for the olfactory processes', *Annals New York Academy of Sciences*, (512), pp. 608–612.

Zohora, S. E., Srivastava, A. K. and Dey, N. (2016) 'Gas Sensing Techniques in Electronic Nose and its Applications : A Review', *EEECOS*, pp. 178–183.